A Numerical Study of a Class of TVD Schemes for Compressible Mixing Layers

N. D. Sandham, Stanford University, Stanford, California
H. C. Yee, Ames Research Center, Moffett Field, California
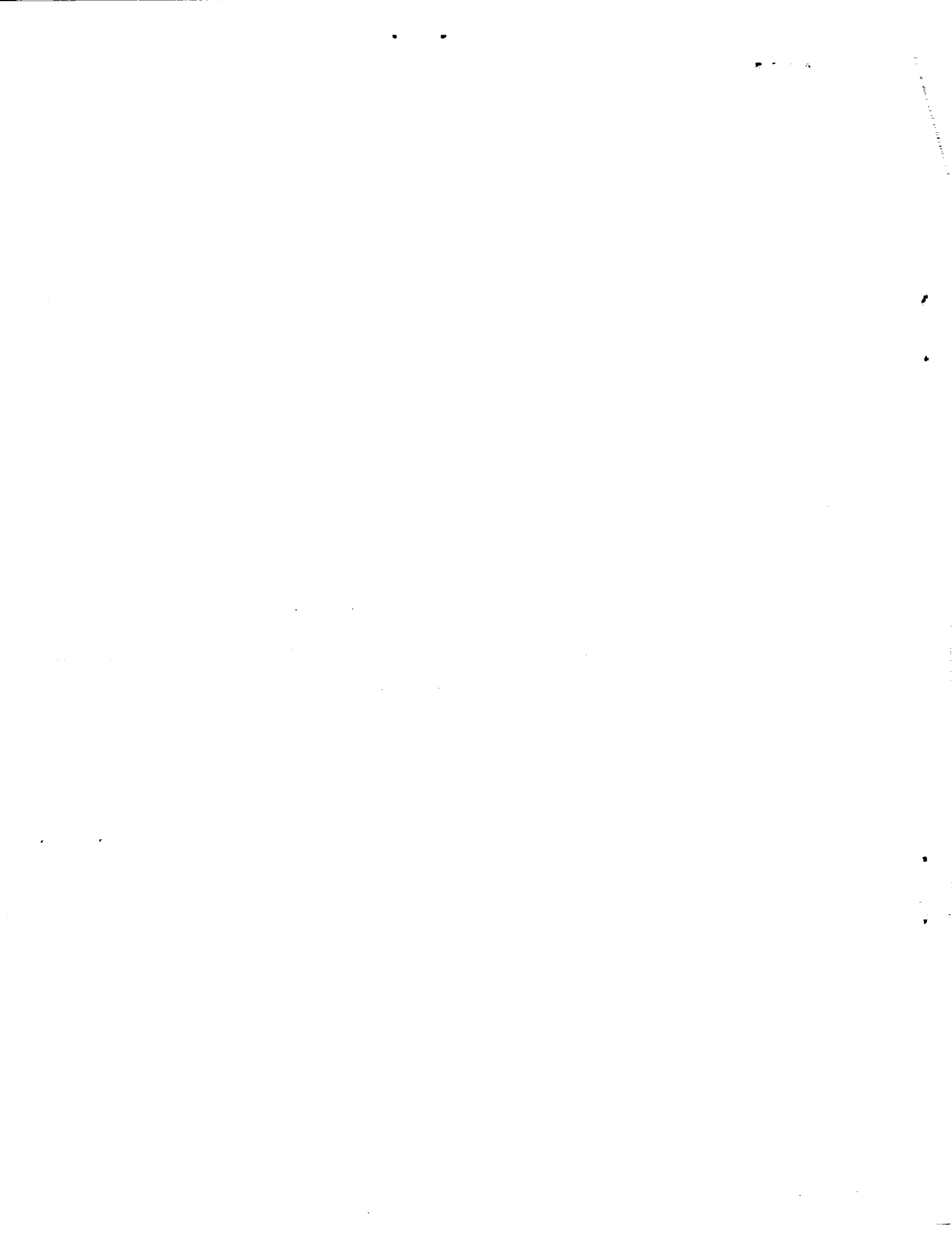
May 1989

A Numerical Study of a Class of TVD Schemes for Compressible Mixing Layers

N. D. Sandham*
Stanford University, Stanford CA 94305

and

H. C. Yee**
NASA Ames Research Center, Moffett Field, CA 94035

Abstract

At high Mach numbers the two-dimensional time-developing mixing layer develops shock waves, positioned around large-scale vortical structures. A suitable numerical method has to be able to capture the inherent instability of the flow, leading to the roll-up of vortices, and also must be able to capture shock waves when they develop. Standard schemes for low speed turbulent flows, for example spectral methods, rely on resolution of all flow-features and cannot handle shock waves, which become too thin at any realistic Reynolds number. The objective of this work is to study the performance of a class of second-order explicit total variation diminishing (TVD) schemes on a compressible mixing layer problem. The basic idea is to capture the physics of the flow correctly, by resolving down to the smallest turbulent length scales, without resorting to turbulence or sub-grid scale modeling, and at the same time capture shock waves without spurious oscillations. The present study indicates that TVD schemes can capture the shocks accurately when they form, but without resorting to a finer grid have poor accuracy in computing the vortex growth. The solution accuracy also depends on the choice of limiter. However a large number of grid points are in general required to resolve the correct vortex growth. This phenomenon in computing time-dependent problems containing shock waves as well as vortical structures is partly due to the inherent shock-capturing property of all TVD schemes. In order to capture shock waves without spurious oscillations these schemes reduce to first-order near extrema and indirectly produce 'clipping phenomena', leading to inaccuracy in the computation of vortex growth. Accurate simulation of unsteady turbulent fluid flows with shock waves will require further development of efficient, uniformly higher than second-order accurate, shock-capturing methods.

---

* Research Assistant, Department of Mechanical Engineering
** Research Scientist, Computational Fluid Dynamics Branch

1. Introduction

Interest in supersonic combustion has led to renewed efforts to understand the physics of high-speed turbulent flows. Mixing in supersonic combustors occurs in compressible free shear layers, where there can be shock waves and large scale vortical structures, which arise from instabilities in the flow. Direct numerical simulations of such flows will greatly aid in understanding compressible turbulence, and modeling mixing and chemical reactions in high speed flows. The two-dimensional time-developing mixing layer is a simple prototype of a free shear layer and has been selected for the current study, where we investigate the merits of a class of TVD shock-capturing methods.

The time-developing mixing layer, shown schematically on figure 1, consists of two streams of fluid moving in opposite directions, with a smooth velocity profile in between. The mean velocity profile has an inflection point and is unstable to small disturbances. The linear stability characteristics of the flow have been presented by Sandham and Reynolds (1989). It was found that compressibility damps the two-dimensional growth of disturbances, and that three-dimensional waves become important at high Mach numbers. The physics of the flow are described in detail in Sandham (1989), where it is shown that there is a range of free-stream Mach numbers around 0.8 where the two-dimensional disturbance is still amplified, leading to a large-scale vortical structure. Flow around this vortex is accelerated to locally supersonic speeds and, in order to reach the stagnation point in between the vortices, has to compress through a nearly-normal weak ($M \approx 1.2$) shock wave. In this flow regime there is an instability to be captured, and shock waves to be handled, which represents a severe test for any numerical method. The approach in Sandham (1989) was to use spectral and high-order Padé finite differences (Lele, 1989) and rely on resolution of all relevant length scales. In order to capture shock waves this meant that low Reynolds numbers had to be used so that, with 7-8 grid points within the shock wave, there are no oscillations around the shock – in fact the computed result is hopefully a full solution of the compressible Navier-Stokes equations, including shock wave structure. Those computations were limited to a small range of Reynolds numbers – high enough so that the instability rolled up strongly enough to form shock waves, but low enough so that the shock waves could be fully resolved. This becomes prohibitively expensive as the Reynolds number is increased, since it is very inefficient to have to resolve the internal shock structure in all the computations. The smallest length scale in the shock wave is of the order of the molecular mean free path, while the smallest turbulent length scale is much bigger than this. For the transitional mixing layer the smallest length scale to be resolved is a Taylor diffusion scale, where strain balances diffusion, while for a general turbulent flow the smallest scale would be of the order of the Kolmogorov scale.

Computations of the compressible mixing layer using TVD schemes were presented by Soestrisno *et al.* (1988), where the inviscid equations were solved. These compu-

tations showed the correct basic structure, but resolution was low. The spatially-developing mixing layer was attempted by Guirguis *et al.* (1987), using an inviscid flux-corrected transport (FCT) method. However the computations were at a very high convective Mach number where the instability is very weakly amplified. The resulting flow fields show low resolution of flow features, indicating that an insufficient number of grid points were used in the computations. For turbulent flow computation, and calculation of mixing, we need to resolve properly the diffusion length scales in the flow.

In this paper we assess the performance of a class of second-order explicit TVD methods for the viscous time-developing mixing layer, and identify the advantages and disadvantages of these methods. The basic idea is to try to resolve down to the smallest turbulent length scales, and so capture the physics of the flow correctly, without resort to turbulence or sub-grid scale modeling, and at the same time capture shock waves without having spurious oscillations.

2. Problem Formulation

The governing equations are the two-dimensional time-dependent Navier-Stokes equations, with no turbulence model.

$$\frac{\partial U}{\partial t} + \frac{\partial F}{\partial x} + \frac{\partial G}{\partial y} = \frac{1}{Re}\left[\frac{\partial F_\nu}{\partial x} + \frac{\partial G_\nu}{\partial y}\right] \tag{1}$$

where U is $(\rho, \rho u, \rho v, e)^T$. The velocity components in the x and y directions are u and v respectively. The density is ρ and the total energy per unit volume is e. F and G are the Euler fluxes in the x and y directions, and F_ν and G_ν are the fluxes due to viscous terms. Re is the Reynolds number of the flow. The complete formulation in generalized coordinates is the same as described in Yee (1987). The mean profiles of velocity and temperature are specified by the following relations:

$$u = 0.5\tanh(2y) \tag{2}$$

$$T = 1 + M^2\frac{(\gamma - 1)}{2}(1 - u^2). \tag{3}$$

The temperature profile satisfies the compressible boundary-layer energy equation, assuming a Prandtl number of unity. The free-stream Mach number is M, and in the current work we assume that the free-streams have equal and opposite velocities and equal temperatures. Pressure is assumed uniform initially so the mean density profile can be obtained directly from the temperature profile. The viscosity μ is assumed to follow Sutherlands Law:

$$\mu/\mu_1 = \frac{(c^2/c_1^2)^{1.5}(1 + 110.3/T_{\text{ref}})}{c^2/c_1^2 + 110.3/T_{\text{ref}}} \tag{4}$$

3

where c is the sound speed, subscript 1 refers to the upper free-stream and the reference temperature T_{ref} is set to 300 K. The various non-dimensional parameters in the flow are the free-stream Mach number, Reynolds number, Prandtl number and Schmidt number. The Reynolds number is based on the initial vorticity thickness of the mixing layer, the velocity difference across the layer, and the free-stream viscosity. The Prandtl number is set to unity, as is the Schmidt number which is required for calculation of diffusion terms in the passive scalar equation that is solved alongside the continuity, momentum and energy equations. The passive scalar is initialized with a hyperbolic tangent profile and tags fluid from each of the free-streams separately, so that mixing of two species in the layer can be visualized.

The flow is periodic in the streamwise direction, x, so periodic boundary conditions are applied. Slip-wall boundary conditions are imposed in the normal direction, y, where a stretched mesh maps the walls to a large enough distance from the centerline that they do not interfere with the computation.

The flow is unstable to small disturbances. This instability is forced, by adding small perturbations, u' and v', to the initial mean flow.

$$u' = \text{amp} \frac{yL}{10\pi} \sin(2\pi x/L) e^{-y^2/10} \tag{5}$$

$$v' = \text{amp} \cos(2\pi x/L) e^{-y^2/10} \tag{6}$$

where 'amp' is the amplitude of the disturbance. The perturbation shape on the normal velocity component in the y direction is made to resemble the linear eigenfunction, and decays to zero in the free-stream. The perturbation in the streamwise velocity is chosen so that the entire disturbance is divergence-free.

In this paper, the disturbance amplitude is chosen to be 0.05 and the wavelength L is set to 20 initial vorticity thicknesses. The Mach number is 0.8 and the Reynolds number 400.

3. Numerical Methods

The Navier-Stokes equations are discretized in conservation law form. The numerical methods are given here only for one space direction, since terms for the other direction are identical. The viscous terms are treated by second-order central differences, and for simplicity of presentation are not included here. Let U_j^n be the solution at grid point j and at time step n, and let Δt be the time step and Δx the grid spacing. A base method, used for comparison purposes, is the explicit MacCormack method:

$$U_j^{(1)} = U_j^n - \lambda(F_j^n - F_{j-1}^n) \tag{7a}$$

4

$$U_j^{n+1} = \frac{1}{2}\left[U_j^{(1)} + U_j^n - \lambda(F_{j+1}^{(1)} - F_j^{(1)})\right] \tag{7b}$$

where $\lambda = \Delta t/\Delta x$. Equation (7) can be modified to have the TVD-type property in a manner described in Yee (1987,1989). These predictor-corrector TVD-type methods for the nonlinear hyperbolic conservation laws (Euler equations) using Roe's approximate Riemann solver can be expressed as:

$$U_j^{(1)} = U_j^n - \lambda(F_j^n - F_{j-1}^n) \tag{8a}$$

$$U_j^{(2)} = \frac{1}{2}\left[U_j^{(1)} + U_j^n - \lambda(F_{j+1}^{(1)} - F_j^{(1)})\right] \tag{8b}$$

$$U_j^{n+1} = U_j^{(2)} + \frac{\lambda}{2}\left(R_{j+\frac{1}{2}}\Phi_{j+\frac{1}{2}} - R_{j-\frac{1}{2}}\Phi_{j-\frac{1}{2}}\right). \tag{8c}$$

When the TVD part (the second term in equation (8c)) is evaluated at $U_j^{(2)}$ the scheme is referred to as PC1 and when it is evaluated at U_j^n it is referred to as PC2. The PC2 method is proven TVD for the scalar constant coefficient case but requires more storage than PC1. See LeVeque and Yee (1988) and Yee (1989) for more details on the behavior of PC1 and PC2. The matrix R is the right-eigenvector matrix of the flux Jacobian $A = \partial F/\partial U$. The specific form used in the current study is shown in Yee (1985). The elements of $R_{j+\frac{1}{2}}$ are determined by Roe's averaging (an approximate Riemann solver), which can be written as follows:

$$u_{j+\frac{1}{2}} = \frac{u_j + Du_{j+1}}{1 + D}, \tag{9a}$$

$$v_{j+\frac{1}{2}} = \frac{v_j + Dv_{j+1}}{1 + D}, \tag{9b}$$

$$H_{j+\frac{1}{2}} = \frac{H_j + DH_{j+1}}{1 + D}, \tag{9c}$$

$$c_{j+\frac{1}{2}}^2 = (\gamma - 1)\left[H_{j+\frac{1}{2}} - \frac{1}{2}\left(u_{j+\frac{1}{2}}^2 + v_{j+\frac{1}{2}}^2\right)\right], \tag{9d}$$

$$\text{where} \quad D = \sqrt{\frac{\rho_{j+1}}{\rho_j}} \quad \text{and} \quad H = \frac{e+p}{\rho}. \tag{9e}$$

For more details of the development of the schemes the reader is referred to Yee (1987,1989). For a symmetric second-order TVD scheme the elements of $\Phi_{j+\frac{1}{2}}$, denoted by $(\phi_{j+\frac{1}{2}}^l)^S$, $l = 1,..,4$ are given by

$$(\phi_{j+\frac{1}{2}}^l)^S = |a_{j+\frac{1}{2}}^l|(1 - \lambda|a_{j+\frac{1}{2}}^l|)(\alpha_{j+\frac{1}{2}}^l - \widehat{Q}_{j+\frac{1}{2}}^l) \tag{10}$$

5

where

$$\alpha_{j+\frac{1}{2}} = R_{j+\frac{1}{2}}^{-1}(U_{j+1} - U_j). \qquad (11)$$

The value $a_{j+\frac{1}{2}}^l$ is the local characteristic speed a^l evaluated at a symmetric average of U_j and U_{j+1}, using equation (9). For the Euler terms considered here the local characteristics are $(u - c, u, u, u + c)$. The following symmetric limiters $\widehat{Q}_{j+\frac{1}{2}}^l$ were tested:

$$\widehat{Q}_{j+\frac{1}{2}}^l = \text{minmod}(\alpha_{j-\frac{1}{2}}^l, \alpha_{j+\frac{1}{2}}^l) + \text{minmod}(\alpha_{j+\frac{1}{2}}^l, \alpha_{j+\frac{3}{2}}^l) - \alpha_{j+\frac{1}{2}}^l, \qquad (12a)$$

$$\widehat{Q}_{j+\frac{1}{2}}^l = \text{minmod}(\alpha_{j-\frac{1}{2}}^l, \alpha_{j+\frac{1}{2}}^l, \alpha_{j+\frac{3}{2}}^l), \qquad (12b)$$

$$\widehat{Q}_{j+\frac{1}{2}}^l = \text{minmod}[2\alpha_{j-\frac{1}{2}}^l, 2\alpha_{j+\frac{1}{2}}^l, 2\alpha_{j+\frac{3}{2}}^l, \frac{1}{2}(\alpha_{j-\frac{1}{2}}^l + \alpha_{j+\frac{3}{2}}^l)], \qquad (12c)$$

where the minmod of two arguments x and y is defined as

$$\text{minmod}(x, y) = \text{sgn}(x)\max\{0, \min(|x|, y\,\text{sgn}(x))\} \qquad (13)$$

with sgn(x)=sign(x). These limiters, equations (12a-c), will be referred to as S1, S2 and S3 respectively in the test calculations.

For a second-order upwind TVD scheme the elements of $\Phi_{j+\frac{1}{2}}$, denoted by $(\phi_{j+\frac{1}{2}}^l)^U$, are

$$(\phi_{j+\frac{1}{2}}^l)^U = -\sigma(a_{j+\frac{1}{2}}^l)(g_{j+1}^l + g_j^l) + [|a_{j+\frac{1}{2}}^l + \gamma_{j+\frac{1}{2}}^l| - \lambda(a_{j+\frac{1}{2}}^l)^2]\alpha_{j+\frac{1}{2}}^l \qquad (14a)$$

where

$$\sigma(z) = \frac{1}{2}(|z| - \lambda z^2) \qquad (14b)$$

and

$$\gamma_{j+\frac{1}{2}}^l = \sigma(a_{j+\frac{1}{2}}^l)(g_{j+1}^l - g_j^l)/\alpha_{j+\frac{1}{2}}^l \qquad (14c)$$

except when $\alpha_{j+\frac{1}{2}}^l = 0$, in which case $\gamma_{j+\frac{1}{2}}^l$ is set to zero. The following upwind limiter functions were tested:

$$g_j^l = \text{minmod}(\alpha_{j-\frac{1}{2}}^l, \alpha_{j+\frac{1}{2}}^l) \qquad (15a)$$

$$g_j^l = (\alpha_{j+\frac{1}{2}}^l \alpha_{j-\frac{1}{2}}^l + |\alpha_{j+\frac{1}{2}}^l \alpha_{j-\frac{1}{2}}^l|)/(\alpha_{j+\frac{1}{2}}^l + \alpha_{j-\frac{1}{2}}^l) \qquad (15b)$$

$$g_j^l = \{\alpha_{j-\frac{1}{2}}^l[(\alpha_{j+\frac{1}{2}}^l)^2 + \delta] + \alpha_{j+\frac{1}{2}}^l[(\alpha_{j-\frac{1}{2}}^l)^2 + \delta]\}/[(\alpha_{j+\frac{1}{2}}^l)^2 + (\alpha_{j-\frac{1}{2}}^l)^2 + 2\delta] \qquad (15c)$$

$$g_j^l = S \cdot \max[0, \min(2|\alpha_{j+\frac{1}{2}}^l|, S\alpha_{j-\frac{1}{2}}^l), \min(|\alpha_{j+\frac{1}{2}}^l|, 2S\alpha_{j-\frac{1}{2}}^l)]; S = \text{sgn}(\alpha_{j+\frac{1}{2}}^l) \qquad (15d)$$

$$g_j^l = \text{minmod}(2\alpha_{j-\frac{1}{2}}^l, 2\alpha_{j+\frac{1}{2}}^l, \frac{1}{2}(\alpha_{j+\frac{1}{2}}^l + \alpha_{j-\frac{1}{2}}^l)). \qquad (15e)$$

In the third limiter the constant δ was chosen to be 10^{-7}.

One can modify the limiter easily to obtain a uniformly second-order non-oscillatory scheme, which can maintain second-order accuracy at extrema. A variation of the total variation bounded (TVB) scheme introduced by Shu (1987) can be obtained (Yee, 1989) by redefining the g_j^l function as

$$
\begin{aligned}
g_j^l &= \frac{1}{2}\text{minmod}(\alpha_{j+\frac{1}{2}}^l, \omega\alpha_{j-\frac{1}{2}}^l + M\Delta x^2 \text{sgn}(\alpha_{j+\frac{1}{2}})) \\
&+ \frac{1}{2}\text{minmod}(\alpha_{j-\frac{1}{2}}^l, \omega\alpha_{j+\frac{1}{2}}^l + M\Delta x^2 \text{sgn}(\alpha_{j-\frac{1}{2}})).
\end{aligned}
\tag{16}
$$

In the current implementation ω was set to 1, and the value of M was chosen to be 50, following the recommendation of Shu from tests using Burgers' equation. No attempt was made to optimize the values of ω and M.

The above upwind TVD limiters, equations (15a-e), will be referred to as U1-U5, and the TVB limiter, equation (16), as U6 in the following sections. Equations (10) and (14) are written in the non-entropy satisfying forms since unsteady computations are involved. These equations can be easily modified to satisfy an entropy inequality (see Yee (1989) for an example).

4. Results

The computations were run with a variable time step, at a CFL number, based on the convective and viscous terms (MacCormack, 1985), of 0.8. The basic grid used for calculation of a single structure was 75×75, when 800 time steps were computed. A uniformly spaced grid was used in the x direction with box length 20, and a geometric stretching was used in the y direction to map the walls to about $y = \pm 50$. For comparison purposes we first present results for the growth of a single vortical structure at $M = 0.8$ on a 75×75 grid, computed using the basic MacCormack method with no artificial dissipation term. A measure of the width of the mixing layer is the vorticity thickness, which is computed based on the mass-weighted velocity profile:

$$
\delta_{\tilde{\omega}} = \frac{\Delta U}{\left| \frac{d(\overline{\rho u}/\bar{\rho})}{dy} \right|_{\text{max}}}
\tag{17}
$$

where $\bar{u}$ and $\overline{\rho u}$ are spatial averages in the homogeneous x direction. The developed structure is shown in contour plots of mixture fraction, density, vorticity and Mach number on figures 2a-d. To assess the accuracy of the various schemes a simulation with a finer grid was made, hereafter referred to as the high resolution run. Contour plots for this case, using a 150×150 grid with symmetric TVD scheme (10) and limiter

7

S3, are shown on figure 3. The growth in vorticity thickness is shown on figure 4. First the small disturbance grows in the linear regime, and the mean flow grows by viscous diffusion. Then the disturbance becomes large and grows non-linearly. It finally saturates out when the structure has filled the computational box and the periodicity constraint prevents it, or any subharmonics, growing any more.

The contour plot for the mixture fraction (figure 2a) shows how fluid from the upper side (solid contours) and fluid from the lower side (dashed contours) have become wrapped around each other. There is a steep gradient formed between the two free-stream fluids in the saddle-point region between two structures. The width of this strained diffusion layer is the characteristic small length scale of this flow. Contour plots of the density and Mach number show that fluid around the top and bottom of the vortical structure is accelerated to locally supersonic speeds (peak Mach number 1.2), and then compresses through nearly-normal shock waves. With the MacCormack method we see the development of oscillations, especially on the downstream side of the shock wave. There is enough natural viscosity in the flow that the MacCormack scheme, with no artificial dissipation term, does not actually fail with the development of these weak shock waves. More accurate methods such as spectral methods, would show strong oscillations at this point.

The growth history of the mixing layer computed using the three symmetric TVD schemes is shown on figure 4, and compared with the MacCormack computation, and with the high-resolution run (150×150, S3). It can be seen that there is a wide variation between the symmetric limiters. We are in a region of the flow physics where the growth rate is very sensitive to the Reynolds number, and any extra damping introduced by the numerical method (or 'clipping' with a TVD scheme) makes a large difference. One could run the simulations at a very high Reynolds number and get less difference between the schemes. However in that case the smallest length scales would not be resolved by the grid, and the numerical scheme itself would be acting as a sub-grid scale model, which defeats the purpose of a direct simulation, where we try to compute all the turbulent scales of motion with no modeling errors. We find that all the symmetric TVD schemes are more dissipative than MacCormack's method (without an added numerical dissipation term), and have lower growth rates and smaller developed structures. The least dissipative limiter is S3 followed by S2 and S1. The developed structure for the S3 limiter is shown on figure 5. The shock wave is well captured in 3 grid points, but the developed structure is smaller than with MacCormack's method. The correct growth for this Reynolds number would lead to a structure even bigger than that obtained with MacCormack's method (c.f. figure 2)

The upwind schemes on a 75×75 grid are compared on figures 6a and 6b. These show different characteristics to the symmetric schemes. The start of the non-linear growth region is reached earlier in time, which agrees with the higher resolution run. However the growth rate in the non-linear region, determined by the slope of the curves

8

at a time of approximately 60, is reduced. In this region the limiter U5 is the least dissipative followed by U2, U3 and U1. In general it was found that the reduction in growth rate was tied to the usual descriptor of limiters as compressive or dissipative: the more compressive the limiter the sharper the shock waves are captured and, in this case, the better the growth rate. The most compressive limiter that was tried was the 'superbee' limiter, U4, which is designed for contact discontinuities. This limiter was found to over-predict the growth rate.

The two methods of implementing the TVD part of the predictor-corrector time advance were investigated. Method PC1 advances the TVD part at the predictor step $U^{(2)}$, while PC2 advances it at step U^n (equation (8)). PC2 is TVD for the scalar constant coefficient case, but requires more storage than PC1. Plots of growth against time are compared on figure 7. At this Mach number there is no significant difference between the methods. At lower Mach numbers it was found that PC2 is slightly more dissipative than PC1.

The cost of the methods, relative to the basic MacCormack method, were assessed for a 75×75 computation run on the Cray X-MP 4/8 at NASA Ames. The symmetric TVD schemes were 17% more expensive than the basic MacCormack method for this problem, and the upwind schemes were 93% more expensive. The reason for the large difference between the upwind and symmetric schemes lies in the ability of the methods to be vectorized on the Cray X-MP. For the symmetric schemes with no entropy correction all conditional statements can be removed from the TVD loops and these vectorize. However the upwind schemes still have to check for a zero in the denominator of equation (14c) and this conditional statement prevents vectorization of the main TVD loop. Note that an arbitrary small parameter can be added to the denominator of (14c) to remove the conditional statement, be we chose to use (14c) to avoid an added parameter. The simulations of the compressible mixing layer without shock waves presented in Sandham (1989) cost about twice as much as the MacCormack method. However those simulations had spectral accuracy, and were fully resolved.

Based on cost and performance for the mixing layer problem the choice of best method is between the symmetric TVD scheme with limiter S3, and the upwind schemes with limiters U5 or U6. The U6 limiter is a TVB scheme with uniform second-order accuracy, and is as good as the best TVD schemes. The upwind schemes U5 and U6 have the best results for a given grid, but in the current implementation cost 65% more.

The effect of resolution for the symmetric scheme was evaluated by running four simulations with grids of 53×53, 75×75, 106×106 and 150×150. The convergence of the upwind schemes is expected to be similar. If the scheme were second-order we would expect the error to decrease by a factor of 2 for each increase in resolution of $\sqrt{2}$. The total cost of the simulations increased by a factor of about 3 with each increase in resolution. Plots of the growth history for each of these cases are shown on figure 8. It can be seen that a large number of points are required if we want to capture all the

9

details of the mixing layer growth correctly. Part of the problem is that of the TVD scheme reducing to first-order at points of extrema. The same problem will affect all TVD, MUSCL (Van Leer, 1974) and FCT methods which attempt to combine a low order dissipative scheme for use around a shock wave, with a high order scheme for smooth regions. It is possible that extra accuracy in smooth regions is not worth the additional cost since the schemes still reduce in order at extrema, though this issue has not been addressed here. Contour plots for the highest resolution case (150 × 150, PC1 with symmetric TVD and limiter S3) are shown on figure 3.

5. Discussion

It is well established that TVD schemes do a good job of capturing shock waves. It was the intention of this study to assess the performance of TVD schemes (10) and (14) in a flow where other physical processes, besides shock waves, need to be captured. The basic finding is that these second-order TVD schemes require very fine grids in order to capture all the flow features in the type of physical problem considered here.

The major drawback with TVD schemes (10) and (14) appears to be the low rate of convergence as the mesh is refined, due to a low global order of accuracy. Other TVD-type methods which attempt to obtain a higher order of accuracy are high order MUSCL (Van Leer, 1974) and FCT (Boris and Book, 1973) schemes. However both these methods obtain higher order by increasing the accuracy of the solution only in smooth regions of the flow. They still reduce to first-order at points of extrema. Hope for future computation of these flows may lie with UNO (Uniformly Non-Oscillatory) and ENO (Essentially Non-Oscillatory) schemes (Harten *et al.*, 1987), which try to fit high-order polynomials through all parts of the flow, including points of extrema. Very impressive results have been obtained with these methods for idealized model problems. However the performance of these schemes on more practical flow problems remains to be seen. The schemes for reconstruction presented by Harten *et al.* (1987) do lose accuracy at points of extrema, unless accompanied by finer grids. It is not clear what the overall gains are, since the operations count and grid stencil for ENO-type schemes are larger than for TVD-type schemes.

Highly accurate numerical methods, such as spectral and Padé schemes, do a very good job of resolving turbulent flow features. However when shock waves are in the flow a prohibitively low Reynolds number, below that needed for resolution of the turbulence, is required in order to resolve the shock waves. Without full resolution these schemes rapidly fail. An artificial viscosity term could be added to these methods, provided that this term does not affect the computation of the turbulent scales. The dissipation due to artificial viscosity, viewed in wave space, would have to be concentrated at wavenumbers higher than the largest turbulence wavenumber.

10

6. Conclusions

A class of second-order explicit Total Variation Diminishing schemes have been evaluated for numerical simulation of the two-dimensional compressible time-developing mixing layer, with the following conclusions:

(1) The best TVD methods were a symmetric scheme with limiter S3 (equation (12c)) and upwind schemes with limiters U5 (equation (15e)) and U6 (equation (16), a TVB scheme). The Upwind schemes gave better results but for the current implementation were 65% more expensive due to less efficient vectorization on the Cray X-MP. Other limiters were more diffusive and it was found that the 'compressive' nature of the limiter was sufficient to predict its performance on the mixing layer problem. The less compressive and more dissipative the limiter, the slower the growth of the mixing layer.

(2) All the methods gave slightly different results, and for this problem it is necessary to use up to 150×150 grid points to properly resolve the growth of a single vortical structure.

(3) At present no ideal numerical method has been found for this flow, which requires high accuracy to resolve the growth of an instability in a viscous regime, and the ability to handle shock waves without oscillations. There is a need for uniformly higher than second-order accurate numerical methods which are efficient and include a shock-capturing capability.

Acknowledgements

References

BORIS, J. P. and BOOK, D. L. 1973, Flux-Corrected Transport. I SHASTA, A Fluid Transport Algorithm That Works. *J. Comp. Phys.* Vol. 11, 38-69.

GUIRGUIS, R. H., GRINSTEIN, F. F., YOUNG, T. R, ORAN, E. S., KAILASANATH, K. and BORIS, J. P. 1988, Mixing Enhancement in Supersonic Free Shear Layers. *AIAA paper* no. 87-0373.

HARTEN, A., ENGQUIST, B., OSHER, S. and CHAKRAVARTHY, S. R. 1987, Uni-

formly High Order Accurate Essentially Non-Oscillatory Schemes, III. *J. Comp. Phys.* Vol. 71, 231-303.

LELE, S. K. 1989, Direct Numerical Simulation of Compressible Free Shear Flows. *AIAA Paper* no. 89-0374.

LEVEQUE, R. J. and YEE, H. C. 1988, A Study of Numerical Methods for Hyperbolic Conservation Laws with Stiff Source Terms. NASA TM-100075, also *J. Comp. Phys.*, to appear.

MacCORMACK, R. W. 1985, Current Status of Numerical Solution of the Navier-Stokes Equations. *AIAA Paper* no. 85-0032.

SANDHAM, N. D. 1989, A Numerical Investigation of the Compressible Mixing Layer. *Ph.D. Thesis*, Mechanical Engineering Department, Stanford University, in preparation.

SANDHAM, N. D. and REYNOLDS, W. C. 1989, The Compressible Mixing Layer: Linear Theory and Direct Simulation. *AIAA Paper* no. 89-0371.

SHU, S.-W. 1987, TVB Uniformly High-Order Schemes for Conservation Laws. *Math. Comp.* Vol. 49, No. 179, 105-121.

SOESTRISNO, M., EBERHARDT, S., RILEY, J. J. and McMURTRY, P. 1988, A Study of Inviscid, Supersonic Mixing Layers Using a Second-Order TVD Scheme. *AIAA Paper* no. 88-3676.

VAN LEER, B. 1974, Towards the Ultimate Conservative Difference Scheme. II. Monotonicity and Conservation Combined in a Second Order Scheme. J. Comp. Phys. Vol. 14, 361-370.

YEE, H. C. 1985, Implicit Total Variation Diminishing (TVD) Schemes for Steady-State Calculations. *J. Comp. Phys.* Vol. 57 no. 3, 327-360.

YEE, H. C. 1987, Upwind and Symmetric TVD Schemes. NASA TM-89464.

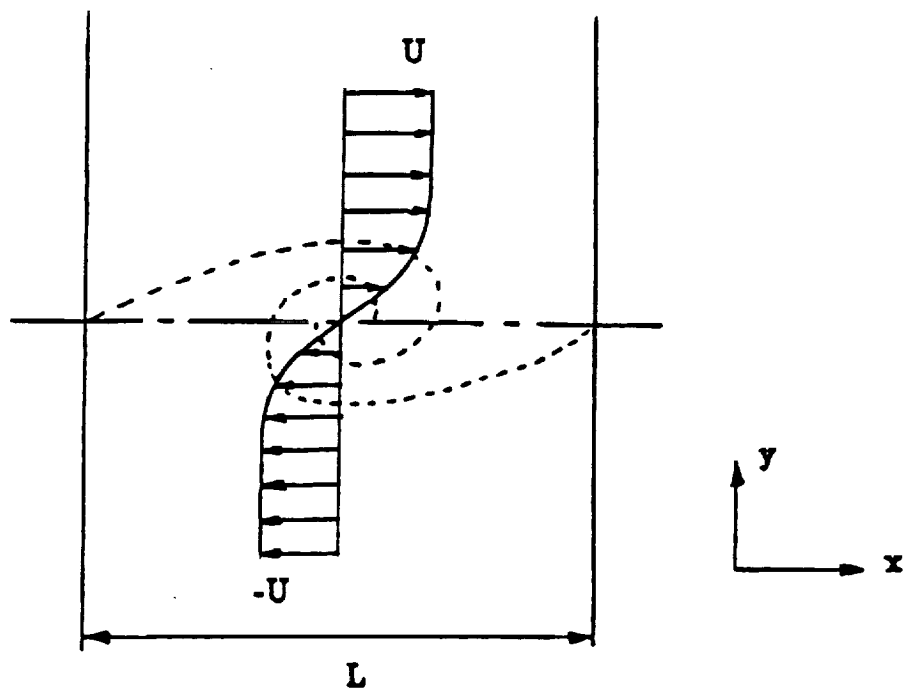YEE, H. C. 1989, A Class of High-Resolution Explicit and Implicit Shock-Capturing Methods. NASA TM-101088.

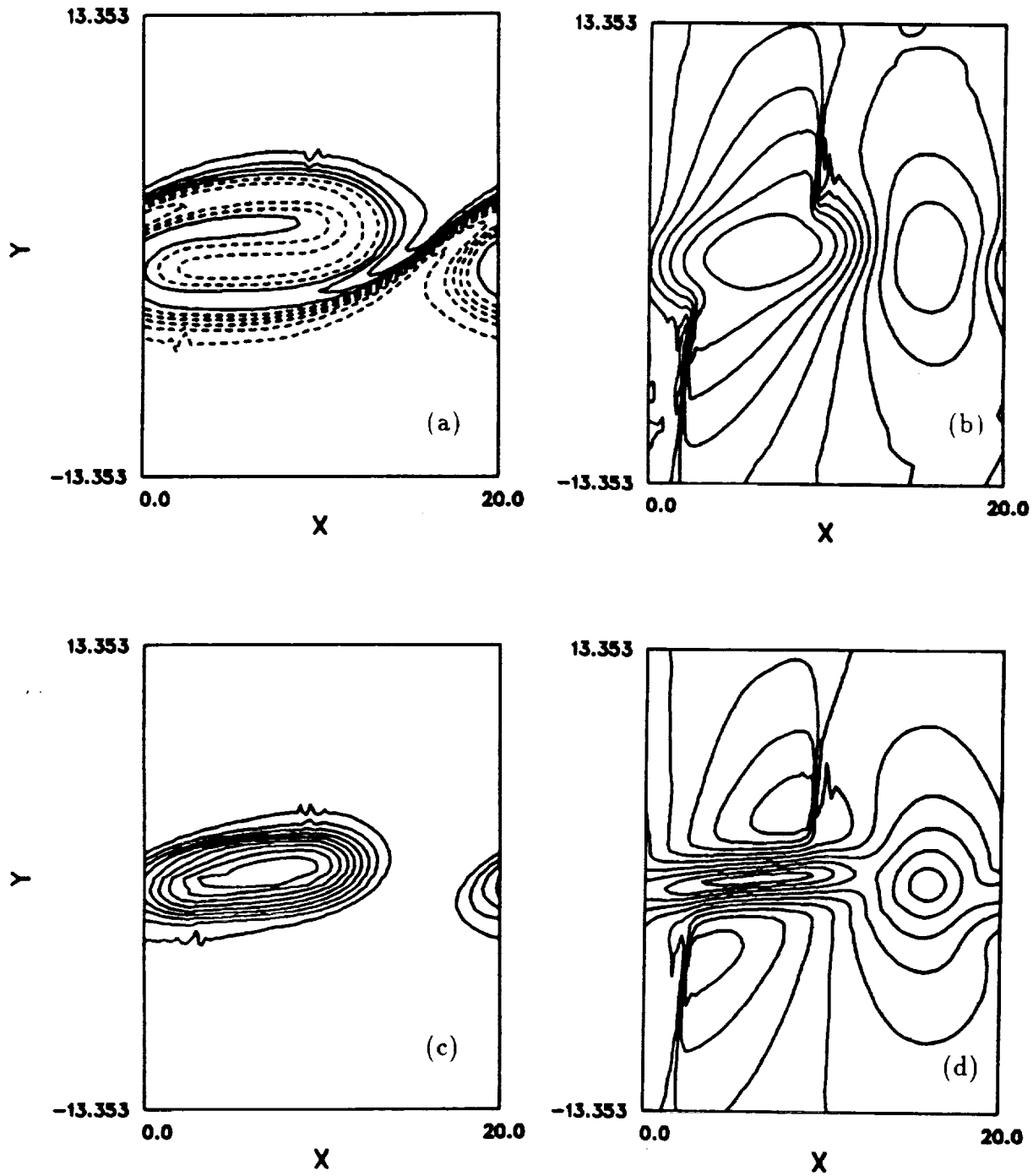Figure 1. Schematic of the time-developing mixing layer.

Figure 2. Flow structure at $M = 0.8$, MacCormack's method using a 75×75 grid: (a) mixture fraction, (b) density, (c) vorticity divided by density and (d) Mach number.
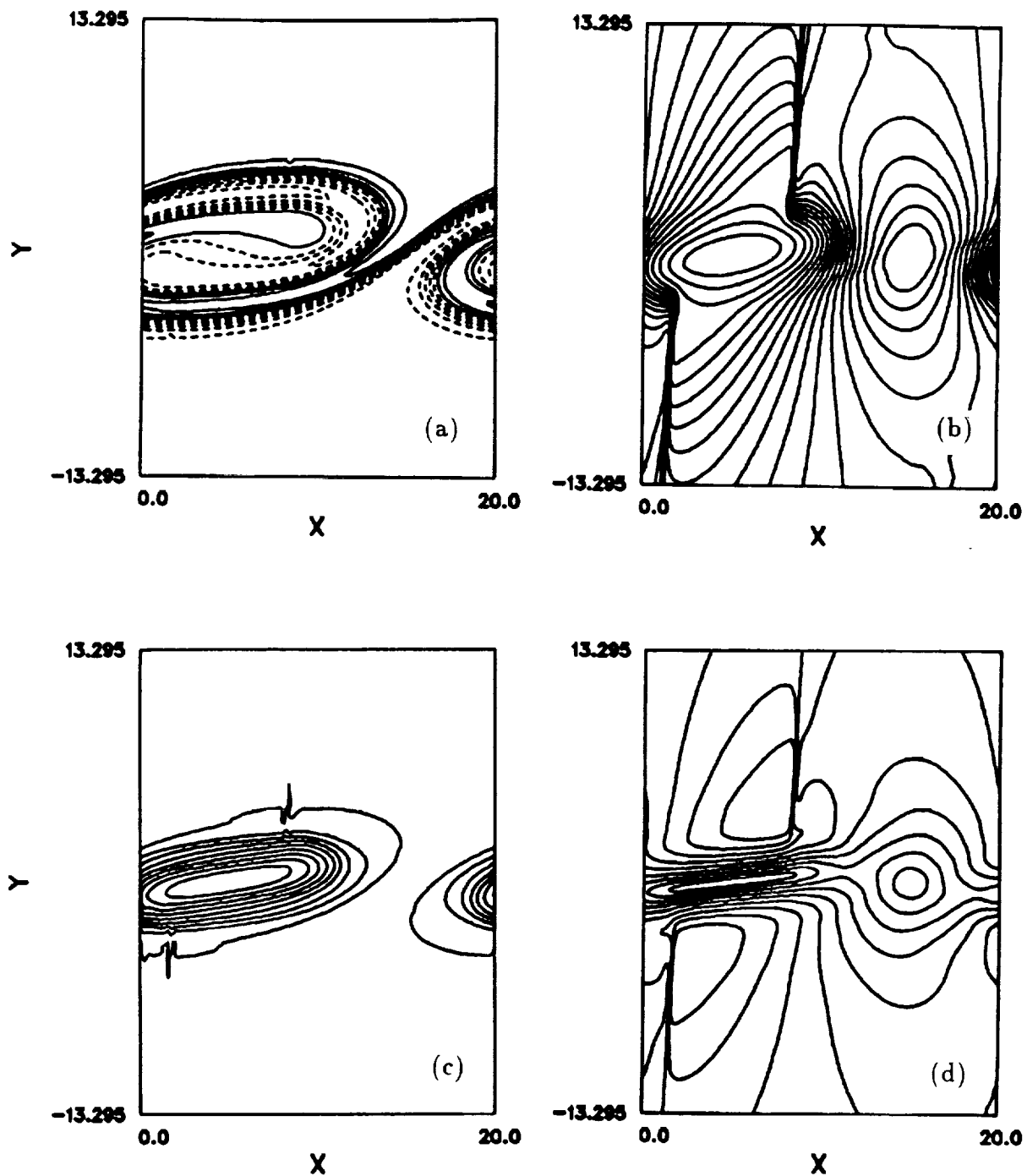
Figure 3. Flow structure at $M = 0.8$, TVD S3 method using a 150×150 grid: (a) mixture fraction, (b) density, (c) vorticity divided by density and (d) Mach number.
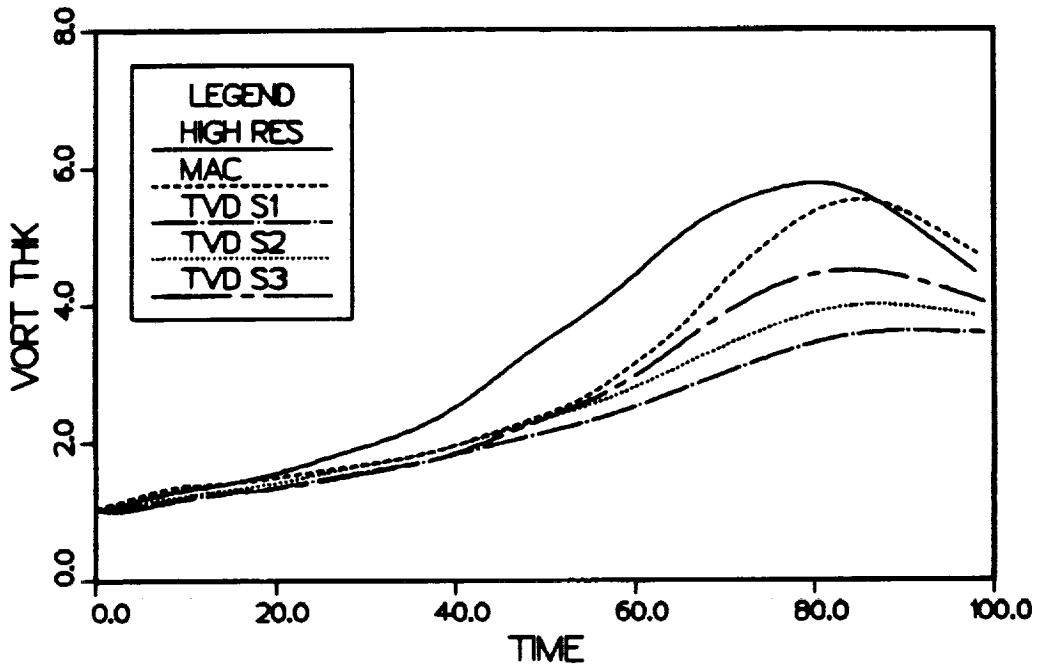
Figure 4. Growth versus time, comparing symmetric TVD schemes on a 75 × 75 grid
with MacCormack method on the same grid, and with a high-resolution run
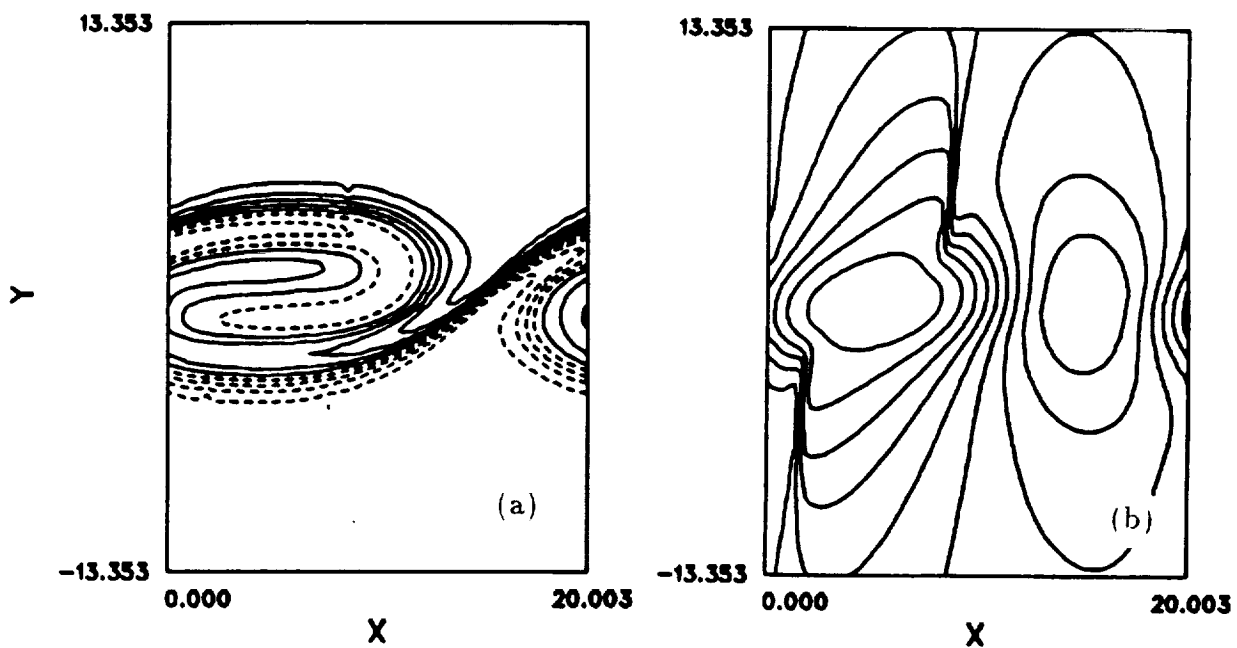on a 150 × 150 grid using the symmetric TVD scheme S3.

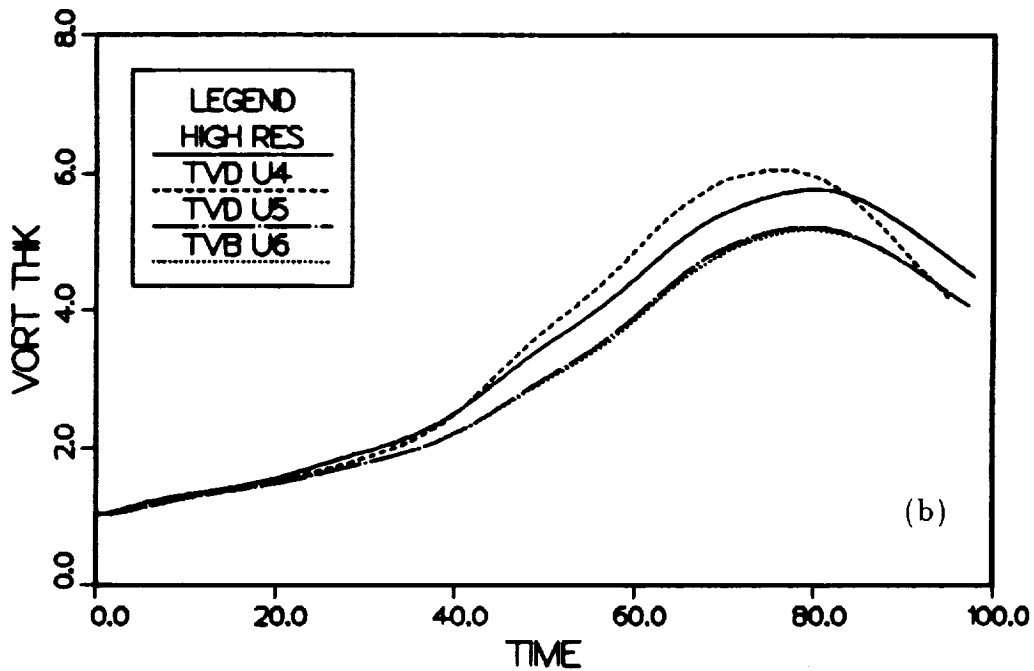Figure 5. Flow structure with S3 limiter on a 75 × 75 grid: (a) mixture fraction and (b) density.
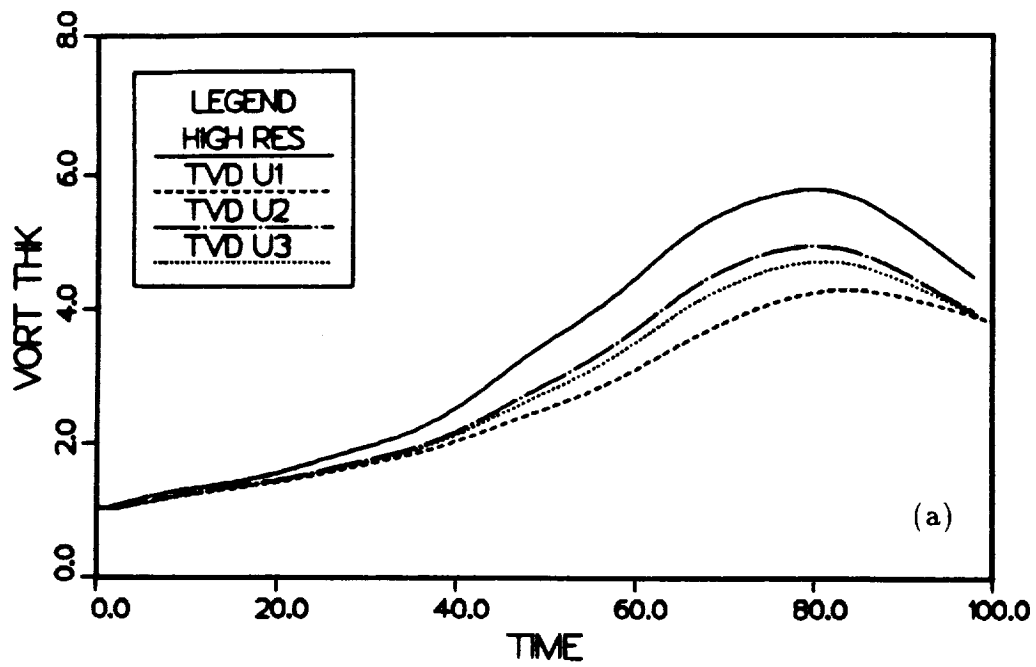
Figure 6. Growth versus time, upwind TVD schemes on a 75 × 75 grid compared with a high-resolution run (*c.f.* figure 4): (a) U1, U2, U3 (b) U4, U5, U6.
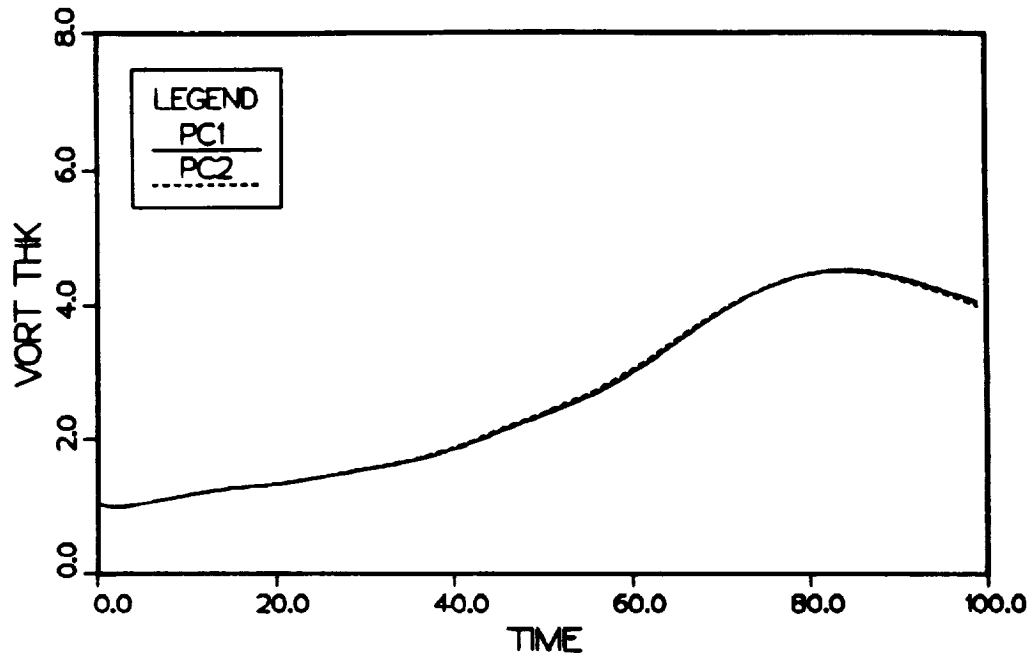
18

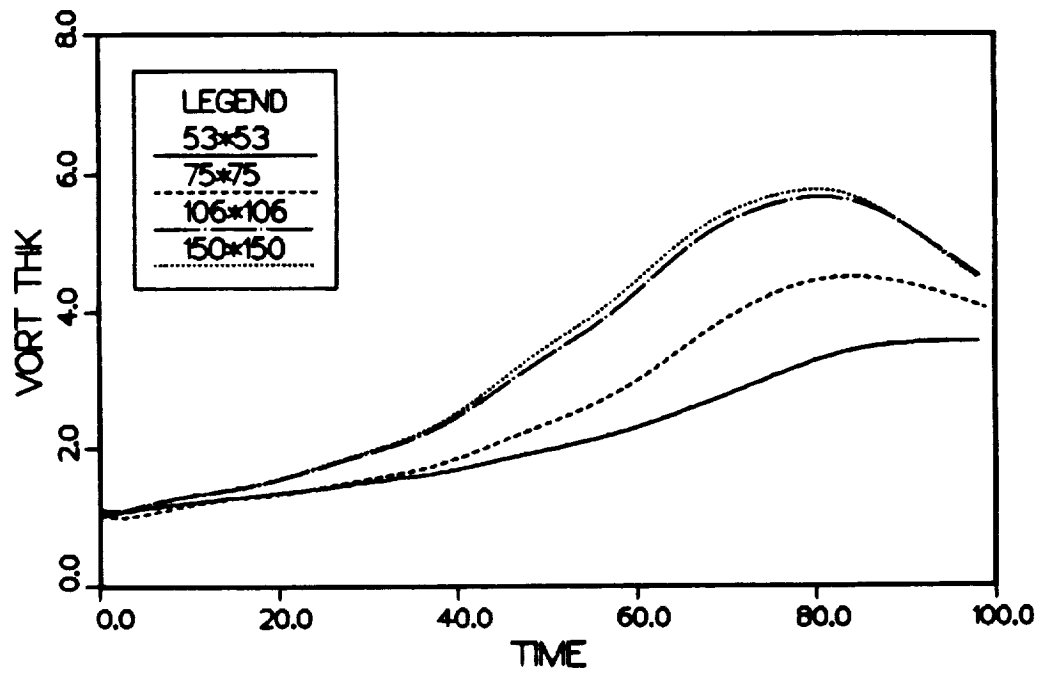Figure 7. Comparison of predictor-corrector methods PC1 and PC2 on a 75 × 75 grid.

Figure 8. Effect of increased resolution on growth (TVD S3 method).

NASA
National Aeronautics and Space Administration

Report Documentation Page

1. Report No. NASA TM-102194	2. Government Accession No.	3. Recipient's Catalog No.

4. Title and Subtitle

A Numerical Study of a Class of TVD Schemes for Compressible Mixing Layers

5. Report Date

May 1989

6. Performing Organization Code

7. Author(s)

N. D. Sandham (Stanford University, Stanford, CA) and H. C. Yee

8. Performing Organization Report No.

A-89139

10. Work Unit No.

9. Performing Organization Name and Address

Ames Research Center
Moffett Field, CA 94035

11. Contract or Grant No.

13. Type of Report and Period Covered

Technical Memorandum

12. Sponsoring Agency Name and Address

National Aeronautics and Space Administration
Washington, DC 20546-0001

14. Sponsoring Agency Code

15. Supplementary Notes

Point of Contact: H. C. Yee, Ames Research Center, MS 202A-1, Moffett Field, CA 94035
(415) 694-4769 or FTS 464-4769

16. Abstract

At high Mach numbers the two-dimensional time-developing mixing layer develops shock waves, positioned around large-scale vortical structures. A suitable numerical method has to be able to capture the inherent instability of the flow, leading to the roll-up of vortices, and also must be able to capture shock waves when they develop. Standard schemes for low speed turbulent flows, for example spectral methods, rely on resolution of all flow-features and cannot handle shock waves, which become too thin at any realistic Reynolds number. The objective of this work is to study the performance of a class of second-order explicit total variation diminishing (TVD) schemes on a compressible mixing layer problem. The basic idea is to capture the physics of the flow correctly, by resolving down to the smallest turbulent length scales, without resorting to turbulence or sub-grid scale modeling, and at the same time capture shock waves without spurious oscillations. The present study indicates that TVD schemes can capture the shocks accurately when they form, but without resorting to a finer grid have poor accuracy in computing the vortex growth. The solution accuracy depends on the choice of limiter. However a larger number of grid points are in general required to resolve the correct vortex growth. The low accuracy in computing time-dependent problems containing shock waves as well as vortical structures is partly due to the inherent shock-capturing property of all TVD schemes. In order to capture shock waves without spurious oscillations these schemes reduce to first-order near extrema and indirectly produce 'clipping phenomena', leading to inaccuracy in the computation of vortex growth. Accurate simulation of unsteady turbulent fluid flows with shock waves will require further development of efficient, uniformly higher than second-order accurate, shock-capturing methods.

17. Key Words (Suggested by Author(s)) Explicit shock-capturing methods Total variation diminishing schemes (TVD) Compressible Mixing layer Turbulent flow	18. Distribution Statement Unclassified-Unlimited Subject Category - 64

19. Security Classif. (of this report) Unclassified	20. Security Classif. (of this page) Unclassified	21. No. of pages 20	22. Price A02